THERMAL BEHAVIOR OF POLY(α-n-ALKYL β-L-ASPARTATE)S

S. Montserrat[1], P. Colomer[1], Y. Calventus[1],
F. López-Carrasquero[3], A. Martínez de Ilarduya[2] and
S. Muñoz-Guerra[2]*

[1]Departament de Màquines i Motors Tèrmics, E.T.S.E.I.T., Universitat Politècnica de Catalunya, Colom 11, E-08222 Terrassa
[2]Departament d'Enginyeria Química, E.T.S.E.I.B., Universitat Politècnica de Catalunya, Diagonal 647, E-08028 Barcelona, Spain
[3]Departamento de Química, Facultad de Ciencias, Universidad de los Andes, Mérida 5101A, Venezuela

Abstract

A series of poly(α-n-alkyl β-L-aspartate)s (n being the number of carbon atoms in the linear alkyl side chain, with n=1, 2, 4, 6, 8, 12, 18 and 22), was studied by differential scanning calorimetry and thermogravimetric analysis. The effect of the length of the alkyl group on thermal properties such as stability, melting and crystallization of side chains, was investigated. For the polymers with $n \geq 12$, two endothermic peaks at T_1 and T_2 were detected separating three distinct phases A, B and C. The peak at T_1 corresponds to the melting of the crystallized paraffinic side chains (transition A–B), and the peak at T_2 may be attributed to a transition (B–C), implying a liquid crystal phase.

Keywords: DSC, helical conformation, poly(α-n-alkyl-L-aspartate)s

Introduction

Poly(α-n-alkyl β-L-aspartate)s are a new family of nylon-3 polymers which are able to adopt helical conformations [1, 2]. The modification introduced in these nylons involved an alkoxycarbonyl group stereoregularly attached to every third backbone carbon atom of the repeating unit as shown in the following general chemical structure:

$$\leftarrow\!\!\!\!\left[NH\text{-}CH\text{-}CH_2\text{-}CO \right]\!\!\!\!\xrightarrow{}_x$$
$$\underset{COOR}{|}$$
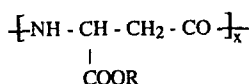
The length of the alkyl group R of the side chain determines the structure and properties of these polymers. In this paper, we study the effect of the length of the

---

* Author to whom all correspondence should be addressed.

side chain on the thermal behavior of poly(α-*n*-alkyl β-*L*-aspartate)s. We will refer to these polyamides as PAALA-*n*, where *n* indicates the number of carbon atoms of the alkyl side chain, being *n* = 1, 2, 4, 6, 8, 12, 18 and 22.

Experimental

Materials

Poly(α-*n*-alkyl β-*L*-aspartate)s studied in this work were prepared by nonassisted anionic ring-opening polymerization of the corresponding optically pure (S)-4-(alkoxycarbonyl)-2-azetidinones [2, 3]. This method allows one to obtain these polymers for a wide range of *n* values with a high degree of stereoregularity and large molecular weights.

Thermal analysis

Calorimetric measurements were performed using a Mettler TA 4000 thermoanalyzer equipped with a low temperature range DSC-30 differential scanning calorimetric module at a heating rate of 10 K min^{-1}, under a nitrogen atmosphere, and calibrated with indium standard. Sample weights of about 6 mg were used. Measurements of sample loss were carried out using a thermogravimetric analyzer TG 50 with a microbalance Mettler M3 coupled to the Mettler TA 4000 equipment.
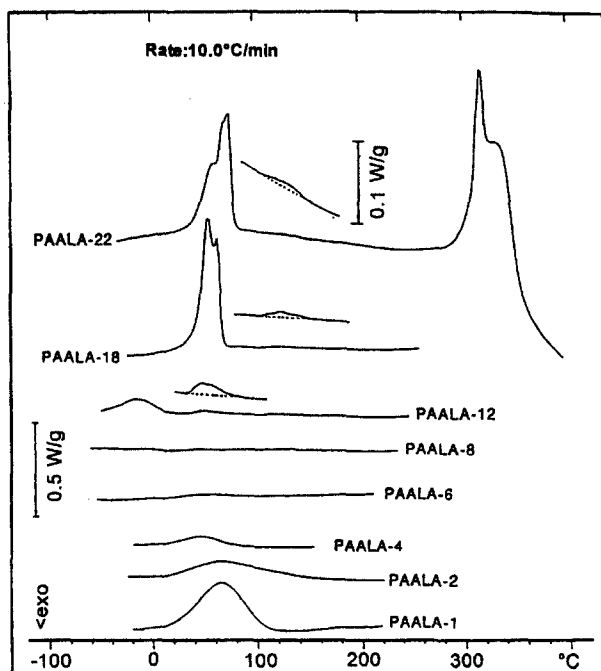

Fig. 1 DSC curves of PAALA-*n* for the indicated values of *n*. Heating rate at 10 K min^{-1}. For PAALA-12, 18, and 22, the transitions at T_2 are enlarged in enclose insets

Similar sample weights were used for these measurements and the non-isothermal thermogravimetric curves were scanned at 10 K min^{-1}.

Results and discussion

Transition temperatures of PAALA-n

DSC scans of PAALA-*n* show two well differentiated regions (Fig. 1). Above 250°C (and shown in Fig. 1 only for PAALA-22), there is an intense endothermic peak which is attributed to the melting and decomposition of the polymer [2, 4]. TG experiments confirm the decomposition by a significant mass loss (Fig. 2). This process is common to the whole family of PAALA-*n* and takes place in two suc- cesive steps involving intramolecular imidation with alcohol elimination and fur- ther scission of the main chain respectively, as shown earlier in reference [2]. De- composition temperatures of PAALA-*n* are shown in Table 1.

In the region below 250°C, the low terms of the series ($n \leq 8$) exhibit a small broad endotherm between 0 and 100°C, the area of which decreases as the length of the alkyl side chain increases becoming almost imperceptible for $n = 6$ and 8. On the other hand, two endothermic peaks, T_1 and T_2 ($T_1 < T_2$), appear in the DSC curves of PAALA-*n* with $n \geq 12$. The first peak, T_1, is much more intense than the second one, T_2. Both peaks tend to shift to higher temperatures as the length of the side chain increases. Thus the T_1 peak appears at –15°C for PAALA-12 and about 75°C for PAALA-22 while the T_2 peak varies from 50 to 129°C. The variation in
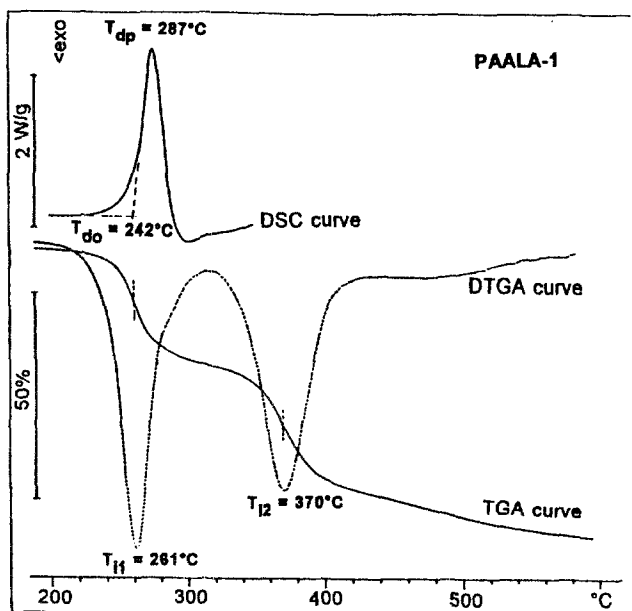

Fig. 2 TG (a) and DSC(b) curves of PAALA-1 in the range of 200–400°C at a heating rate of 10 K min^{-1}. Derivatized plot of TG curve showing the two decomposition steps (c)

Table 1 Physical and thermal properties of poly(α-n-alkyl β-L-aspartate)s studied in this work

R	$M_v \times 10^{-5}$	$T_1^a/$	$\Delta H_{T_1}/$	$T_2^a/$	$\Delta H_{T_2}/$	$T_{d_o}^b/$	$T_{d_p}^b/$	$T_{i_1}^c/$	$T_{i_2}^c/$
		°C	J g^{-1}	°C	J g^{-1}	°C			
CH$_3$	5.8	63	87	–	–	242	287	261	370
C$_2$H$_5$	5.3	67	37	–	–	260	310	261(312)	368
C$_4$H$_9$	3.7	55	8	–	–	195	242	286	377
C$_6$H$_{13}$	2.1	–	–	–	–	275	307	291	384
C$_8$H$_{17}$	4.4	–	–	–	–	318	341	326	380
C$_{12}$H$_{25}$	4.2	–15	17	50	2	325	348	333	380[d]
C$_{18}$H$_{37}$	2.0	54, 64	79	117	1.3	315	330	324	380[d]
C$_{22}$H$_{45}$	≈2	60, 75	86	129	1	305	316	335	380[d]

[a] For $n \geq 12$, T_1 and T_2 correspond to the peak temperatures of transitions A–B and B–C, respectively

[b] T_{d_o} and T_{d_p} are the onset and peak temperatures of the melting-decomposition process measured by DSC

[c] T_{i_1} and T_{i_2} are temperatures at the inflexion points in TG curves which correspond to the peaks in the derivatized curve

[d] very weak inflexion

enthalpy, $\Delta H_{(T_1)}$, associated with the endothermic process at T_1 also increases with the length of the side chain varying from 17 to 86 J g^{-1}. On the other hand, the $\Delta H_{(T_2)}$ associated with the peak at T_2 is smaller, about 1–2 J g^{-1}, being practically insensitive to composition. The temperatures and ΔH values obtained for the PAALA-n series are shown in Table 1.

These results agree with those reported for poly(γ-n-alkyl α-L-glutamate)s with side chains of similar lengths [5, 6]. By analogy with them, the transition at T_1 may be attributed to the melting of the alkyl side chains leading to a partially disordered phase where the helical structure is still retained. The weak endotherm observed at T_2 could be related to a rearrangement undergone by the structure generated at T_1. In PAALA-n with $n \geq 12$, three phases, A, B and C with their existence domains defined by the corresponding temperatures T_1 and T_2 can be differentiated. The structural changes implied in such transitions and their dependence with temperature have been confirmed by X-ray diffraction measurements and solid state NMR [4]. The absence of these melting process for PAALA-6 and -8 is interpreted as a consequence of the short length of the side chain which is not able to crystallize by itself. A previous thermodynamic study of the transition at T_1 showed that the approximate numbers of crystallized methylenes in PAALA-12, 18, and 22 were around 2, 8 and 12 respectively, and consequently the length of the paraffinic chains in PAALA-6 and -8 are not long enough to generate crystallized side chains [4]. On the other hand, the origin of the transition which appears in PAALA-1, -2 and -4 is not clear. Small structural changes not detectable by X-rays are thought to be behind such a transition.

Peak multiplicity of the T_1 endotherm for the A–B transition

The thermal process underlying T_1 is richly complex and strongly dependent on both the side chain size and the thermal history of the polymer. The DSC curve of an "as prepared" sample of PAALA-18, obtained by precipitation from solution, shows the transition at T_1 as a double peak with maxima at 54 and 64°C, the latter appearing as a shoulder on the former. In contrast, three peaks with similar intensities and maxima at 60, 70 and 75°C were observed for PAALA-22 and a broad peak centered around –15°C is found for PAALA-12. Conversely, for all the PAALA witn $n{\geq}12$, only one crystallization peak was observed on cooling and only a single broad endotherm reappeared when the sample was immediately reheated.

The origin of peak multiplicity at T_1 was investigated in detail for the case of PAALA-18 by following the evolution of the endotherm with the thermal history of the polymer. For this, the sample was heated at 110°C for 5 min, rapidly cooled to the annealing temperature T_a below T_1 and maintained there for a period of time, t_a. The heating curves registered after treatment at different values of t_a and T_a are shown in Fig. 3 (a) and (b) respectively, illustrating the opposite effect that anneal-
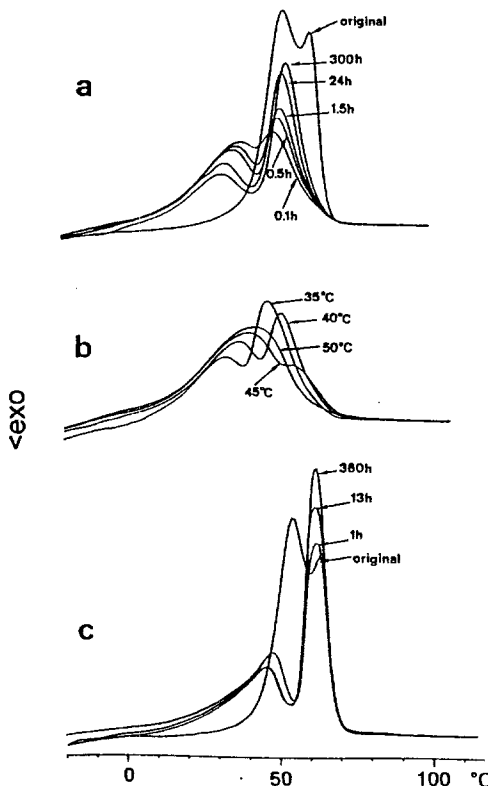

Fig. 3 Effect of temperature and time of annealing on the evolution of T_1 endotherm for the A–B transition in PAALA-18. Sample cooled from 110°C and annealed (a) at 40°C for different periods of time and (b) for 30 min at different temperatures. "As prepared" sample annealed at 50°C for the indicated periods of time (c)

ing has on the double peak. As either the temperature or the time of treatment increases, the two peaks move apart and the enthalpy of the higher temperature peak (T_1^2) increases at the expense of the other. As seen in Fig. 4, the position and height observed for each peak as well as the enthalpy of the whole endotherm show an approximate linear dependence on $\log t_a$ with a slope increasing with T_a. These results lead to the interpretation of the transition at T_1 as a melting process involving crystallites of different dimensions; at a given T_a, a fraction of the side chains crystallizes with a perfection that increases with t_a, the remaining material crystallizing into less well formed crystallites on cooling. A similar increasing in crystallite perfection with annealing has been reported for poly(γ-*n*-octadecyl-α-*L*-glutamate) [6], although the splitting of the double peak is less apparent in this case.
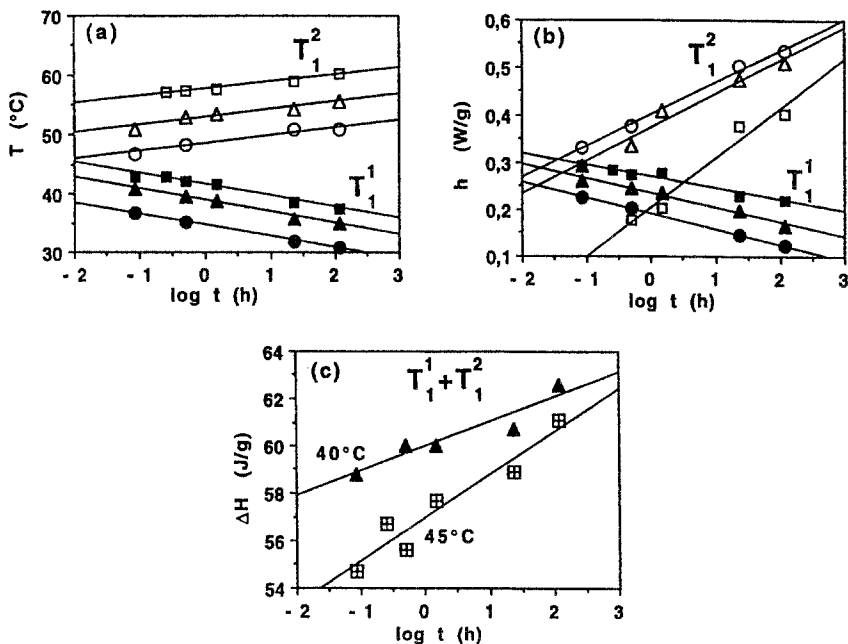
Fig. 4 Variation of the position (a) and height (b) of the two peaks of the T_1 endotherm for the A–B transition in PAALA-18 as a function of the annealing time at different temperatures: 35°C (●, ○); 40°C (▲, △); 45°C (■, □); filled and open symbols refer to lower (T_1^1) and higher (T_1^2) temperature peak respectively. Increase of the total change of enthalpy, ΔH, involved in the transition at different annealing temperatures: 40°C (▲) and 45°C, (□) (c)

The fact that two peaks are observed instead of a broad one is better explained in terms of the different number of methylenes being accommodated in the crystallites. The fact that perfection attainable by annealing is always lower than that existing in the polymer obtained by precipitation from solution is consistent with such as interpretation. Annealing of the precipitated polymer at 50°C for different periods of time shows the increase in enthalpy of the second peak while remaining at the same temperature (T_1^2) (Fig. 3c). In this case, the crystallinity of the sample

could be still increased by annealing but the crystallite size could not be further augmented. A similar effect has been widely reported for certain paraffinic polymers as also is the case of low density polyethylene [7].

The B–C transition at T_2

The transition at T_2 appears in PAALA-12, -18 and -22 as a process taking place after the fusion of the crystallized paraffinic side chains. The transition implies a very small absorption of heat which appears to be practically independent of the side chain length. This transition was difficult to detect in the reheating curve, although it became restored after annealing at T_a for a sufficient period of time, as shown in Fig. 5. Furthermore, the enthalpy involved in this transition was further increased by annealing at temperatures between T_1 and T_2. Since this behavior parallels that reported for the B–C transition in poly(γ-*n*-alkyl-*L*-glutamate)s by Watanabe *et al.* [5] for $n \geq 10$ and by Romero *et al.* [6] for poly(γ-stearyl-α-L-glutamate), it should be interpreted in similar terms; specific side-by-side chain interactions operating in phase B are removed when T_2 is reached and a nematic liquid crystal phase is generated. In fact, X-ray diffraction experiments show a contraction in the lateral spacing of the structure at T_2 indicating that the layered structure of the molten side chains has been abandoned. Optical microscopy observations further support the idea that a cholesteric-nematic rearrangement is implied in the transition B–C in PAALA-18 [2].
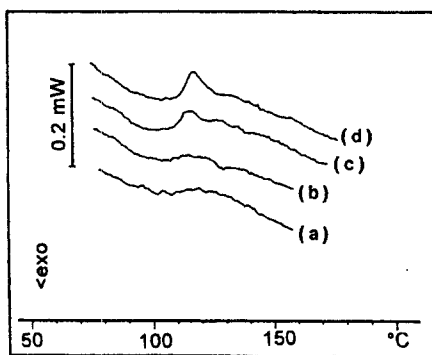

Fig. 5 Transition at T_2 for PAALA-18: (a) first scan on the "as prepared" sample, (b) second scan immediately after the first scan, and (c) and (d) are the scans after annealing of 2 and 24 h, at 100°C, respectively

## Non-isothermal crystallization for the B–A transition

Non-isothermal crystallization taking place at the B–A transition has been studied in PAALA-18 and PAALA-22. The samples were heated from 10 to 120°C at 10 K min^{-1} and left at this temperature for 5 min. Then, the samples were cooled at a constant rate ranging between 2.5 and 20 K min^{-1} from 55 to –10°C for PAALA-18 and from 70 to –15°C for PAALA-22 in order to crystallize the molten

paraffinic side chains. The peak temperature, T_{P_c}, and the crystallization enthalpies, ΔH_c, obtained at different cooling rates are shown in Table 2. In this Table, it may be observed that ΔH_c for PAALA-22 is greater than that corresponding to PAALA-18 as may be expected for the higher number of methylene units in the side chains which participate in the crystalline structure. The crystallized fraction, α, at T_{P_c}, changes with the cooling rate, β, from 0.25 (at –5 K min^{-1}) to 0.33 (at –20 K min^{-1}) for PAALA-18 and from 0.17 (at –5 K min^{-1}) to 0.28 (at –20 K min^{-1}) for PAALA-22.

Table 2 Temperatures of crystallization peak maximum, T_{P_c}, and crystallization enthalpies, ΔH_c at different cooling rates, β

β/ K min^{-1}	PAALA–18		PAALA–22	
	T_{P_c}/°C	ΔH_c/J g^{-1}	T_{P_c}/°C	ΔH_c/J g^{-1}
2.5	41.1	45.9	57.8	65.6
5	39.7	49.7	56.8	70.3
7.5	37.8	50.1	56.2	69.8
10	36.9	49.9	55.4	69.0
12.5	36.8	52.5	54.6	69.9
15	35.4	51.9	53.4	69.2
20	33.1	52.1	52.5	70.8

The apparent activation energy, E_a, for the whole crystallization process is calculated by both Kissinger [8] and isoconversional [9] methods. The values of E_a obtained by the isoconversional method, for α in the range 0.2–0.6, are indicated in Fig. 6. The average value is also indicated in Fig. 6 and is in good agreement with
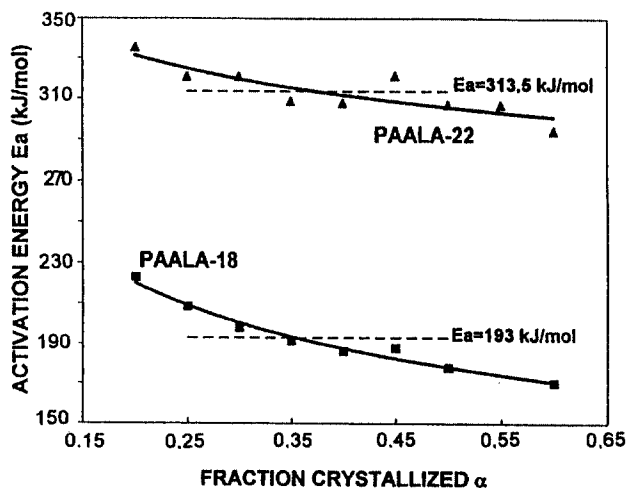
Fig. 6 Apparent activation energy obtained by the isoconversional method for α comprised between 0.2 and 0.6. Dashed lines indicate the corresponding average values

that obtained by the Kissinger equation (212 kJ mol^{-1} and 329 kJ mol^{-1} for PAALA-18 and PAALA-22, respectively). The higher value of E_a observed in PAALA-22 is a logical consequence of the greater mobility of the side chains.

From the DSC curves, the fractions of crystalline material, α, and the transformation rate, dα/dt, have been obtained. The Johnson-Mehl-Avrami-Erofe'ev (JMAE) model has been considered in order to describe the crystallization kinetics of PAALA-18 and PAALA-22. One way to determine the Avrami exponent n that best reproduces experimental results is to use the Ozawa method [10]. By this means the exponent, n, is given by the slope of $\ln(-\ln(1-\alpha))$ *vs.* $\ln\beta$ plot assuming that there is a linear correlation between $\ln K(T)$ and T, $K(T)$ being the kinetic factor related to the apparent activation energy through Arrhenius behaviour. In our case, this requirement is not satisfied and values of n obtained in this way are meaningless (less than 1). Hence, in order to determine the exponent, n, the following equation based on the kinetic equation is used [11]:

$$\mathrm{d}\alpha/\mathrm{d}t = nk^{1/n}(1-\alpha)[-\ln(1-\alpha)]^{(n-1)/n}$$

In Fig. 7 $\ln \mathrm{d}\alpha/\mathrm{d}t$ is plotted *vs.* $-\ln(1-\alpha)$ or the experimental curves and for the theoretical model for $n=1$ and $n=2$.
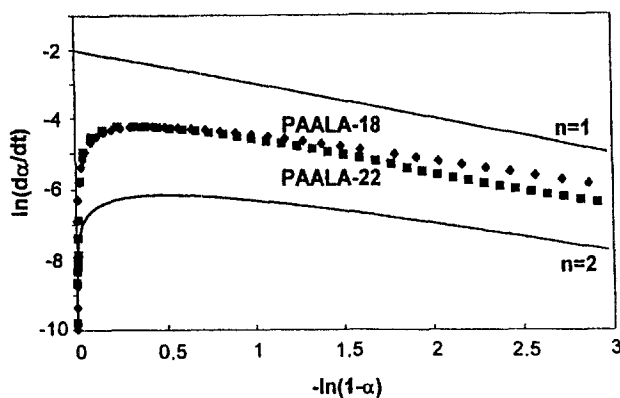

Fig. 7 Plot of $\ln(\mathrm{d}\alpha/\mathrm{d}t)$ *vs.*$-\ln(1-\alpha)$. Experimental curves obtained at a cooling rate of 20 K min^{-1} are represented by symbols: PAALA-18 ($\blacklozenge$) and PAALA-22 ($\blacksquare$). Solid lines are the theoretical curves for $n=1$ and $n=2$

Results show a value of $n=2$ in the complete range of α for PAALA-18 and $n=2$ until $\alpha=0.7$ and $n<2$ for $\alpha>0.7$ for PAALA-22 independently of the cooling rate. These values indicate that a two-dimensional growth crystallization mechanism from preexisting nuclei takes place in both cases.

Conclusions

This paper shows that the thermal behavior of PAALA-*n* is very dependent on the length of the side chain. Above 250°C, all the polymers show a melting-decomposition with a significant mass loss which involves intramolecular imidation with

elimination of alcohol. In the region below 250°C, PAALA-*n* with $n \geq 12$ show three structural phases, A, B, and C, involving two phase transitions. Transition A–B corresponds to the melting of the alkyl side chain, and transition B–C is related to the interconversion of two liquid crystal phases. The crystallization mechanisms of PAALA-18 and -22 were analysed using the JMAE model which showed that two-dimensional growth of preexisting nuclei occurred for both samples. The melting and crystallization enthalpies increase with *n*, corresponding to the increasing number of methylene units in the side chains that form part of the paraffinic phase.

* * *

References

1 J. Fernández-Santín, J. Aymamí, A. Rodriguez-Galán, S. Muñoz-Guerra and J. A. Subirana, Nature (London), 311 (1984) 53.
2 F. López-Carrasquero, M. García-Alvarez and S. Muñoz-Guerra, Polymer, 35 (1994) 4502.
3 M. García-Alvarez, F. López-Carrasquero, E. Tort, A. Rodríguez-Galán and S. Muñoz Guerra, Synthet. Comm., 24 (1994) 745.
4 F. López-Carrasquero, S. Montserrat, A. Martínez de Ilarduya and S. Muñoz-Guerra, Macromolecules, 28 (1995) 5535.
5 J. Watanabe, H.Ono, I. Uematsu and A. Abe, Macromolecules, 18 (1985) 2141.
6 F. J. Romero Colomer, J. L. Gómez Ribelles, J. Lloveras and S. Muñoz Guerra, Polymer, 32 (1991) 1642.
7 P. Colomer, S. Montserrat, M. A. Ribes, J. M. Meseguer, J. L. Gómez and R. Díaz, Polym. Plast. Technol. Eng., 28 (1989) 635.
8 H. E. Kissinger, Anal. Chem., 29 (1957) 1702.
9 H. L. Friedman, J. Polym. Sci. Part C, 6 (1964) 183.
10 T. Ozawa, Polymer, 12 (1971) 150.
11 D. W. Henderson, J. Thermal Anal., 15 (1979) 325.